

THE FUNCTION OF THE DISTANCE OF A CURVE FROM ITS CENTROID IN OPTIMAL SYNTHESIS OF A FIVE-BAR LINKAGE

Jacek Buśkiewicz

Poznan University of Technology
Poznan, Poland
fax: 48 061 665 2307
jacek.buskiewicz@put.poznan.pl

Abstract

A functional description of a closed curve, applied in computer image processing and pattern recognition, is adapted to optimal synthesis of 2-DOF planar five-bar mechanism. The function is the distance of a curve from its centroid (DCC). In the applicable form the DCC is represented by normalized coefficients of its expansion into Fourier series. On the basis of the DCC a new function is defined, which itself is invariant under affine transformations. A distance norm in the sense of the affinity of two curves is introduced. The norm is applied as an objective function in the problem of mechanism synthesis carried out by the genetic algorithm.

Key words:

five-bar linkage, mechanism synthesis, Fourier coefficients, closed curves.

1 Introduction

In general mechanism synthesis is aimed at designing a mechanism so that it realizes specific technological tasks. Nonetheless, at the level of the design it is possible to optimize dynamical features of the mechanism. The paper does not deal directly with the dynamics, but the formulation of a synthesis problem may involve constraints on the range of the transmission angle to minimize the forces transmitted by the links.

Synthesis of a linkage as the path generator is one of the most important and intensively investigated problems of mechanism theory. Graphical methods came into being at earliest [Artobolovski, 1977; Mayourian, and Freudenstein, 1984]. Analytical methods, though being developed, were restricted to few problems due to high complexity [Sandor and Erdman, 1984]. Nowadays the synthesis is carried out with the use of probabilistic (neural networks [Vasiliu and Yannou, 2001] and evolutionary algorithms [Kunjur and Krishnamuty, 1995; Cabrera, Simon and Prado, 2002; Laribi, Mlika, Romdhane and

Zeghloul, 2004]) and deterministic (gradient) methods. The optimization process consists in minimizing an objective function, i.e. a distance between the prescribed and generated curves. But comparison of the desired and generated curves point to point has many disadvantages [Ullah and Kota, 1997]. The satisfactory results are obtained when a complex function describing the curve is expanded into Fourier series and normalized [Ullah and Kota, 1997, Vasiliu, Yannou, 2001; McGarva and Mullineux, 1993; McGarva, 1994]. The same procedure may be applied to the properties of curves as: cumulative angular function or curvature [Zahn and Roskies, 1972; Lu and Kota, 2002] expressed in a functional form. Well-known and wide-used procedures of a normalization of the Fourier series expansion reduce the description to the sequence of numbers. The distance norm between two curves is expressed in terms of the normalized Fourier coefficients. These methods allow minimizing the number of optimized variables and, which is related to it, the cost and time of numerical calculation.

A lot of methods of the shape description are elaborated for purposes of computer image processing and pattern recognition [Kindratenko, 2003; Chanussot, Nystro and Sladoje, 2005]. One of them is adapted in the present paper to the path synthesis problem. The function describing a closed curve is the distance of the curve from its centroid (DCC). The mathematical assumptions and normalization procedures are given, so that the description is invariant under rotation, scaling, mirror reflection, change of the direction, number of points defining the curve and choice of a starting point. This makes the method suitable for constructing an objective function being a measure of the distance between two curves in the sense of the affinity instead of the sense of closeness on the plane. Moreover, the features of the DCC enable constructing an objective function without referring to the harmonic analysis.

The applicability and effectiveness of the function is verified by the results of the optimal synthesis of 2-

DOF planar five-bar mechanism executed by the genetic algorithm.

2 The DCC function description

It is assumed only the continuity of a closed curve with the clockwise orientation given parametrically $(x(s), y(s))$, $s \in (0, L)$, where $s = \widehat{AB}$ is the length of the curve arc measured from the starting point A to any point B, L is the total curve length. Introducing the natural parameter $s^* = \frac{s}{L}$, the normalized curve length equals 1. The centroid (x_c, y_c) is expressed as:

$$x_c = \frac{\int_0^L x(s) ds}{L}, \quad y_c = \frac{\int_0^L y(s) ds}{L}. \quad (1)$$

The distance of the curve from its centroid (the DCC function) referred to the curve length is defined as follows:

$$f(s^*) = \frac{\sqrt{(x(s^*) - x_c)^2 + (y(s^*) - y_c)^2}}{L}. \quad (2)$$

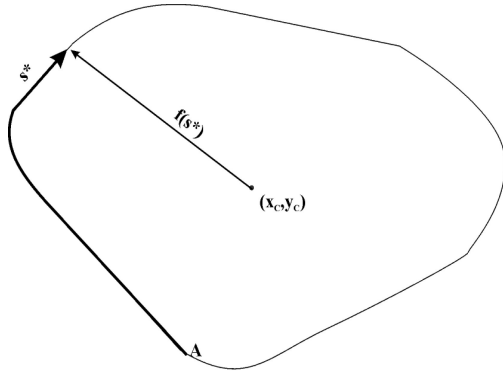


Figure 1. A plane closed curve and its DCC function f .

The DCC function is expanded into the Fourier series

$$f(s^*) = a_0 + \sum_{n=1}^{\infty} (a_n \cos(2n\pi s^*) + b_n \sin(2n\pi s^*)) \quad (3)$$

with coefficients (FCs)

$$a_0 = \int_0^1 f(s^*) ds^*, \quad (4.1)$$

$$a_n = 2 \int_0^1 f(s^*) \cos(2n\pi s^*) ds^*, \quad (4.2)$$

$$b_n = 2 \int_0^1 f(s^*) \sin(2n\pi s^*) ds^*. \quad (4.3)$$

The DCC function can be alternatively expanded into the polar form of the Fourier series

$$f(s^*) = a_0 + \sum_{n=1}^{\infty} A_n \cos(2n\pi s^* + \alpha_n) \quad (5)$$

$$\text{where: } A_n = \sqrt{a_n^2 + b_n^2}, \quad \cos \alpha_n = \frac{a_n}{\sqrt{a_n^2 + b_n^2}},$$

$$\sin \alpha_n = \frac{-b_n}{\sqrt{a_n^2 + b_n^2}}.$$

It is obvious that rotation by an angle, translation, scaling and mirror reflection do not change the DCC function as well as the FCs.

The change of the starting point and reversal of the direction require more penetrating analysis. The normalization of the FCs is done to provide their invariance under these transformations.

The phase angles α_n only undergo the normalization since the harmonic amplitudes A_n are invariant under the considered transformations.

The invariance with respect to the shift of the starting point is ensured by bringing to zero the first non zero harmonic. Provided it is the j -th harmonic, the phase angles are modified as follows:

$$\alpha'_n := (\alpha_n - n\Delta\alpha), \quad n = 1..k, \quad (6)$$

where $\Delta\alpha = \frac{\alpha_j}{j}$. The phase angles α_n are brought

to the interval $(0, 2\pi)$ for each n . The polar expansion of the DCC \tilde{f} of the anticlockwise curve has the form

$$\begin{aligned} \tilde{f}(\tilde{s}^*) &= f(-s^*) = a_0 + \sum_{n=1}^k A_n \cos(-2n\pi s^* + \alpha_n) = \\ &= a_0 + \sum_{n=1}^k A_n \cos(2n\pi s^* - \alpha_n). \end{aligned} \quad (7)$$

The coefficient a_0 does not change whereas the phase angles α_n differ with signs. If for the clockwise curve $\alpha_n = \alpha_0 > 0$, for the anticlockwise curve $\tilde{\alpha}_n = -\alpha_0$ and the substitution $\tilde{\alpha}_n = -\alpha_0 + 2\pi$ brings the angle to $(0, 2\pi)$. As the substitution $\tilde{\alpha}_n = -\alpha_0 + 2\pi$ is allowed, it may be applied to all the angles $\alpha_n > \pi$ bringing them to $(0, \pi)$.

Once the curve is given by a sequence of m points P_i of the coordinates (x_i, y_i) , the set f_i of the values of the DCC function is obtained

$$f_i = f(s_i^*) = \frac{\sqrt{(x_i - x_c)^2 + (y_i - y_c)^2}}{L}, \quad (8)$$

where: $L = \sum_{i=1}^m |P_i P_{i+1}|$, $P_{m+1} = P_1$, $s_i^* = \frac{\sum_{j=2}^i |P_{j-1} P_j|}{L}$ for each $i=1..m$. The centroidal coordinates are approximated numerically as follows:

$$x_C = \frac{\sum_{i=1}^m \frac{x_{i+1} - x_i}{2} \Delta s_i}{L}, y_C = \frac{\sum_{i=1}^m \frac{y_{i+1} - y_i}{2} \Delta s_i}{L}, \quad (9)$$

where $\Delta s_i = |P_i P_{i+1}|$.

A closed curve may be considered as the polygonal curve, then the DCC function may be defined as the continuous function.

The DCC function is approximated by p first terms of the Fourier expansion (Eq. 5). The rectangular rule is applied to the integrals Eqs. (4.1-4.3), yielding the numerical approximation of the FCs.

$$\begin{aligned} a_0 &= \sum_{i=1}^m f(s_i^*) \Delta s_i^*, \\ a_n &= 2 \sum_{i=1}^m f(s_i^*) \cos(2n\pi s_i^*) \Delta s_i^*, \\ b_n &= 2 \sum_{i=1}^m f(s_i^*) \sin(2n\pi s_i^*) \Delta s_i^*. \end{aligned}$$

Then, the FCs are normalized as it is described in this section.

3 Geometric and kinematic analysis of the 2-DOF five-bar mechanism

Most synthesis methods are tested on the four bar-linkage. Many of them are restricted to this mechanism only. In the paper the 2-DOF five-bar linkage is chosen for some purposes: a proposed objective function is checked on synthesis of more miscellaneous paths and for greater number of optimized variables, the particular case of the considered mechanism is the four-bar linkage. The practical applications early motivated the study in the field of synthesis of five bar mechanisms [Rose, 1961; Pollitt, 1962]. In order to synthesize a precise path generating mechanism the five-bar linkage is integrated with gears [Mundo, Gatti and Dooner, 2007] giving, in fact, the mechanical system of single DOF.

The mechanism consists of four moveable links, the active links are indexed as 1 and 3. Then, the angles α_1, α_3 are known at each time. Having given the lengths, the other angles α_2, α_4 are sought for. The path is traced out by the point D. The geometric and kinematic analyses are preceded by checking the conditions for the full-rotatability [Ouyang, 2002; Feng G., Xiao-Qiu Z., Yong-Sheng Z. and Hong-Rui W, 1996].

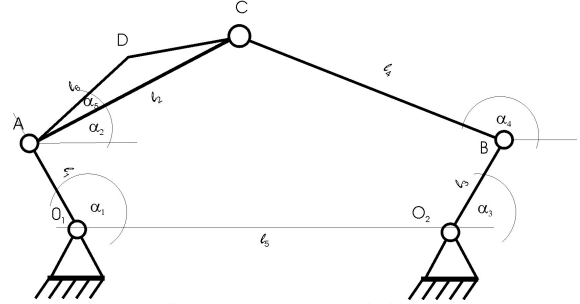


Figure 2. 2-DOF five-bar mechanism with the point D tracing out paths.

Firstly, the position of the point $C(x, y)$ is determined. The lengths of the links 2, 4 are

$$(x - x_A)^2 + (y - y_A)^2 = l_2^2, \quad (10.1)$$

$$(x - x_B)^2 + (y - y_B)^2 = l_4^2. \quad (10.2)$$

where the coordinates of the points A and B are: $x_A = l_1 \cos \alpha_1$, $y_A = l_1 \sin \alpha_1$, $x_B = l_5 + l_3 \cos \alpha_3$, $y_B = l_3 \sin \alpha_3$.

Subtracting Eqs. (10.2) from Eqs. (10.1) gives the equation of a straight line

$$k_3 x + k_4 y = k_1 - k_2, \quad (11)$$

where: $k_3 = 2(x_A - x_B)$, $k_4 = 2(y_A - y_B)$, $k_1 = l_2^2 - (x_A^2 + y_A^2)$, $k_2 = l_4^2 - (x_B^2 + y_B^2)$. Substituting $k_6 = \frac{k_1 - k_2}{k_4}$, $k_5 = -\frac{k_3}{k_4}$ into Eq. (11), it may be written down as

$$y = k_5 x + k_6. \quad (12)$$

Two cases are possible:

(a) $k_4 \neq 0$.

Eq. 12 is substituted into Eq. 10.1, which gives the quadratic equation

$$Kx^2 + Lx + M = 0, \quad (13)$$

with the coefficients: $K = 1 + k_5^2$,

$$L = 2k_5 k_6 - 2y_A k_5 - 2x_A, \quad M = -2y_A k_6 + k_6^2 - k_1.$$

Assuming that $\Delta = L^2 - 4KM \geq 0$, two positions of the point C are possible

$$x_{1,2} = \frac{-L \pm \sqrt{\Delta}}{2K}, \quad y_{1,2} = k_5 x_{1,2} + k_6 \quad (14)$$

(b) $k_4 = 0$.

In both possible configurations the point C lies on the same vertical line. Then, substituting

$$x = x_1 = x_2 = \frac{k_1 - k_2}{k_3} \quad \text{into Eqs. (10.1) gives the quadratic equation}$$

quadratic equation

$$Ny^2 + Py + R = 0, \quad (15)$$

with the coefficients $N = 1$, $P = -2y_A$, $M = x^2 - 2x_Ax + k_1$. When $\Delta = P^2 - 4NR > 0$

$$y_{1,2} = \frac{-P \pm \sqrt{\Delta}}{2N}. \quad (16)$$

Having determined the coordinates of the point C, the unknown angles are computed as follows

$$\alpha_{21,2} = \arctg\left(\frac{x_{1,2} - x_A}{y_{1,2} - y_A}\right), \quad (17.1)$$

$$\alpha_{41,2} = \arctg\left(\frac{x_{1,2} - x_B}{y_{1,2} - y_B}\right). \quad (17.2)$$

The position of the coupler point D is specified by the following kinematic equations:

$$x_D = l_1 \cos \alpha_1 + l_6 \cos(\alpha_2 + \alpha_5), \quad (18.1)$$

$$y_D = l_1 \sin \alpha_1 + l_6 \sin(\alpha_2 + \alpha_5). \quad (18.2)$$

4 The Genetic algorithm description

The genetic algorithm (GA) with the objective function built by means of FCs (Eq. 19) is applied to solve the problem of the mechanism synthesis.

The objective function

The following objective function is proposed

$$E_{A\alpha} = |a_0 - a'_0| + \sum_{n=1}^p (|A_n \cos \alpha_n - A'_n \cos \alpha'_n|) + \sum_{n=1}^p (|A_n \sin \alpha_n - A'_n \sin \alpha'_n|) \quad (19)$$

Where a_0, A_i, α_i and a'_0, A'_i, α'_i are the FCs of curves being compared. Such a form of the objective function reduces the differences between the values of the amplitudes and phase angles, which might have influence on the result when the objective function was taken as

$$E_{A\alpha} = \sum_{n=1}^p (|A_n - A'_n| + |\alpha_n - \alpha'_n|). \quad (20)$$

The scheme of the algorithm

In accordance with the nomenclature of the evolutionary algorithms the single mechanism is an individual, its optimized features are the lengths l_2, l_3, l_4, l_5, l_6 , the initial angle of the link 3 α_{3S} , the angle α_5 and the angular velocities ω_1, ω_3 . Only integer values of ω_1, ω_3 divided by their greatest

common divisor are allowed. The length of the link 1 $l_1 = 1$. The link 1 is connected with the frame at the origin and the immovable link is horizontal.

The population is a set of all the mechanisms. In each successive population the individuals are sorted in the increasing objective function (the fitness is reciprocal of the objective function). The best individual is the first parent for all new individuals, the second parents are selected at random. The feature of a new individual is taken over from the best individual with probability p_b . The features of the new individual are mutated.

For the needs of the genetic algorithm the following parameters are taken:

- the number of individuals N_{\max} (the size of population),
- the number of individuals to be crossed over in each generation l_{cr} ,
- the number of individuals to be randomly generated in each generation.

The algorithm itself does not involve any special improvements, and as a tool widely-used and well-known in mechanism theory is not described in depth. The only enhancement consists in introducing to each population l_{ran} ($l_{ran} < N - l_{cr}$) randomly generated individuals set instead of the worst fitted ones. Then, along with the improvement of the best individual, the whole working space is searched through. It prevents the algorithm getting stuck in any local minima. Moreover, the mutation coefficient is being decreased while the rate of the optimization process does not change in a specified number of iterations.

5 Numerical experiments

The objective of the analysis is to determine the rate of the convergence to the required solution, the similarity of both the required and generated curves, the computational cost for finding the best solution, the uniqueness of the assignment of the function to curves.

To demonstrate the effectiveness of the method the numerical experiments are performed on the following test curves (Figs. 3, 6).

Triangle given by the set of points (x,y)

$$x = \{1.0 \ 2.0 \ 3.0 \ 4.0 \ 5.0 \ 6.0 \ 7.0 \ 6.0 \ 5.0 \ 4.0 \ 3.0 \ 2.0 \ 1.0 \ 0.0 \ 0.0 \ 0.0 \ 0.0 \ 0.0\},$$

$$y = \{0.0 \ 0.0 \ 0.0 \ 0.0 \ 0.0 \ 0.0 \ 0.0 \ 0.0 \ 1.0 \ 2.0 \ 3.0 \ 4.0 \ 5.0 \ 6.0 \ 7.0 \ 6.0 \ 5.0 \ 4.0 \ 3.0 \ 2.0 \ 1.0\}.$$

EllipseArc - The curve is traced out from $t = 0$ to $t = 0.5$ and then back to the starting point $t = 0$ along the same path. As a result self-overlapping closed curve is produced.

$$x(t) = 3 \cos\left(\frac{\pi}{6} + 2\pi t\right), \quad y(t) = 2 \sin\left(\frac{\pi}{6} + 2\pi t\right),$$

$$t \in (0, 0.5).$$

CurveA - The curve is given parametrically

$$x(t) = 5(\cos(4\pi t) + \sin(\pi t)) \quad y(t) = 3 \sin(4\pi t),$$

$$t \in (0, 1).$$

CurveB - The curve is given parametrically

$$x(t) = 5 \cos^3(2\pi t), \quad y(t) = 5 \sin^3(2\pi t), \quad t \in (0,1).$$

Many numerical experiments showed that the normalized area enclosed by the curve makes a significant contribution to improving the efficiency of the algorithm (the accuracy of the approximation, computational cost). The normalized area is computed as follows:

$$A^* = \frac{\sum_{i=1}^{m-1} (x_i y_{i+1} - x_{i+1} y_i) + (x_m y_1 - x_1 y_m)}{L^2} \quad (21).$$

Hence, the formula for the error (Eq. 19) is completed by adding the new term $|A_0^* - A_0^*|$. A^* is of the same order of magnitude as the coefficients A_n . For example for a circle of radius R it is $A^* = A_0 = \frac{R}{2}$; $A_n = 0, n > 0$.

The following parameters are taken as input for the GA.

- The number of individuals $N_{\max} = 55$.
- The number of individuals to be crossed over in each generation $l_{cr} = 35$.
- The number of individuals to be randomly generated in each generation $l_{ran} = 30$.
- The probability of choosing the feature of the best individual while crossing $p_b = 0.75$.

The intervals of optimized parameters:

$$l_2, l_3, l_4, l_5 \in (1, 20), \quad l_6 \in (0, 20),$$

$$\alpha_{3S} \in (0, 2\pi), \quad \alpha_5 \in (0, 2\pi),$$

$$\omega_1 \in (-3, 3), \quad \omega_3 \in (-2, 2).$$

The parameters of the mechanisms generating the curves closest to the desired ones and the errors $E_{A\alpha}$ are collected in Table 1.

The number of the FCs p is taken equal to 5. To precisely estimate the higher harmonics (Eq. 5) appropriately large number of points defining a curve is required. The numerical experiments show that for curves given by 20-40 points, a good approximation is obtained for the first $p = 4, 5, 6$ harmonics. The total number of iterations performed does not exceed at any example 10000. As can be seen from Figs. 3, the degree of the similarity of the test and generated curves is satisfactory. Whenever the numerical algorithms were executed the high degree of repeatability of the results was obtained. In order to best fit found curves to the test curves in general case they have to be translated, scaled, reflected against Y-axis and rotated. It is done by a translation of the centroids of both curves to the same point and adjusting its centroidal axes, which is not here discussed in detail [Dibakar and Mruthyunjaya, 1999].

Table1
The dimensions of the mechanisms generating the approximations of the test curves with the errors $E_{A\alpha}$.

	Triangle	CurveA	CurveB
l_2	11.06	14.22	17.762
l_3	4.897	2.367	15.73
l_4	14.05	19.8797	5.33
l_5	12.03	16.311	2.29
l_6	3.587	8.2622	3.167
α_{3S}	5.61	2.751	3.265
α_5	4.079	3.98345	1.854
ω_1	1	2	3
ω_3	-1	-1	-1
$E_{A\alpha}$	0.01909	0.00303	0.01583

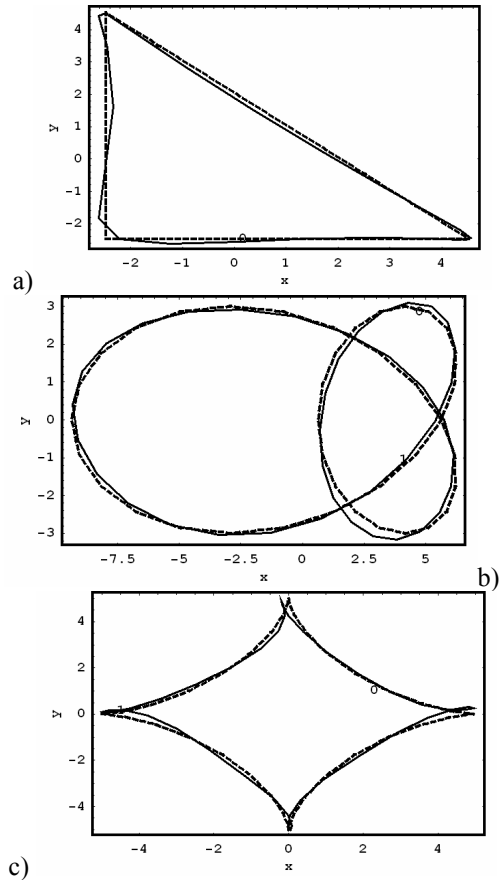


Figure 3. The test curves (dashed line - 0) and the curves generated by the DCC method (continuous line - 1) (a) the triangle, (b) CurveA, (c) CurveB.

Fig 4 shows the typical progress of the convergence process of the synthesis carried out by DCC method. In most cases the first 2000 – 3000 iterations allows localizing an area in nine-dimensional space containing the final solution. The fastest convergence rate is observed in the 1000 initial iterations and further iterations gradually improve the best solution, which can be supported by decreasing the mutation and disturbance coefficients.

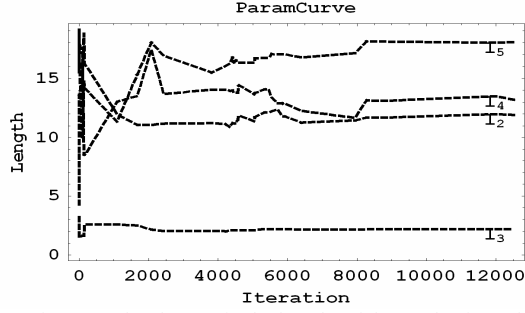


Figure 4. The changes in the lengths of the mechanism while converging to the best solution on the example of synthesis of the *CurveA*.

For illustrative purposes the NFCs of the DCC functions of the *CurveA* and of its best approximation are collected in Table 2. The DCC function, its approximation by the Fourier series truncated to 5 harmonics as well as the normalized function for this curve are drawn in Fig. 5.

Table 2
The NFCs of the DCC function for the *CurveA* and its best approximation obtained.

nr	The DCC method			
	Test curve - <i>CurveA</i>		Generated curve	
	A_n	$\alpha_n (\alpha_0 = A^*)$	A_n	$\alpha_n (\alpha_0 = A^*)$
0	0.09193	0.03296	0.09208	0.03289
1	0.02844	0	0.02811	0.00000
2	0.01681	0	0.01672	0.00256
3	0.04017	0	0.04014	0.00782
4	0.01264	3.14159	0.01152	3.11166
5	0.00516	0	0.00507	0.19222

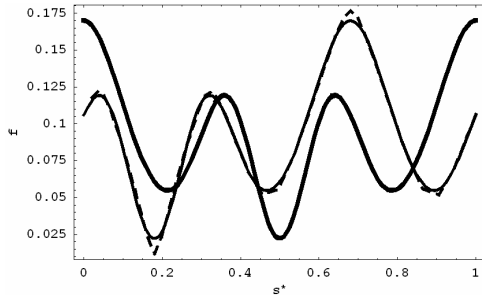


Figure 5. The normalization of the *CurveA* - The DCC function (dashed line), the DCC function approximated by 5 FCs (thin line), the normalized DCC function (thick line).

6 Non-Fourier curve description

A function $F(r)$ built on the base of the DCC function may be assigned to a closed curve. The value of the function F at the point r is equal to the total normalized length of all the arcs $P_{i1}P_{i2}$ of the curve meeting the condition: for any point $P \in P_{i1}P_{i2}$ its distance from the curve centroid $|CP|$ is less than r . $F(r)$ itself is invariant under affine transformations and does not require any normalization (Fig. 6).

$$F(r) = \sum_i P_{i1}P_{i2}, \forall_i \forall_{P \in P_{i1}P_{i2}} |PC| \leq r \quad (22)$$

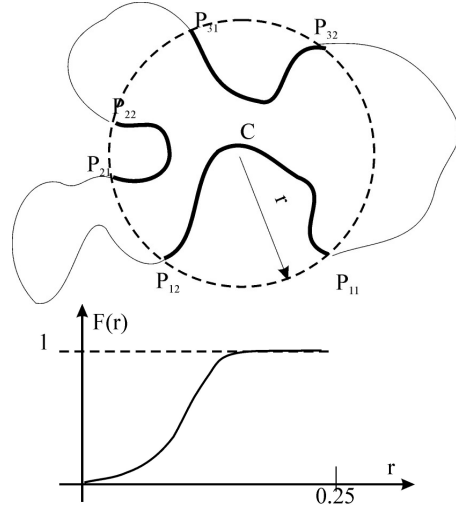


Figure 6. Description of a closed curve in terms of the $F(r)$ function.

It is easy to prove that the maximum value of the argument r for a closed curve (of normalized length equal to 1) is 0.25, as it is for a self-overlapping straight line. There exist many curves of the same function F . Exemplary curves of the same F are shown in Fig. 7. Nonetheless, the preliminary studies show that the function may be successfully applied in mechanism synthesis.

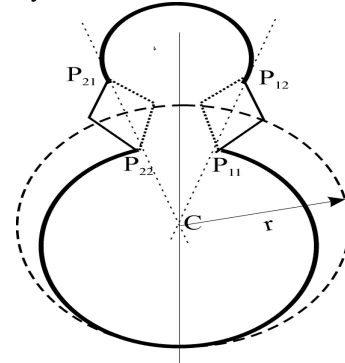


Figure 7. Two curves (I, II) of the same F -function which vary with the lines $P_{11}P_{12}$ and $P_{21}P_{22}$. The paths from the points P_{11} to P_{12} and from P_{22} to P_{21} go along continuous (curve I) or dashed lines (curve II).

For practical applications the function F takes values in a discrete set of arguments. Then, the error between two curves 1,2 is expressed as follows:

$$E_F = \sum_{i=1}^m |F_1(r_i) - F_2(r_i)| \quad (23)$$

The algorithm based on the F -function is applied in synthesis of the ellipsarc curve. It is taken $m = 20$ in the objective function (23). The resultant curve fitted on the ellipsarc is shown in Fig.8. The parameters of the mechanism generating the curve are: $l_2=13.804$, $l_3=1.3845$, $l_4=14.0369$, $l_5=14.5505$, $l_6=3.4117$, $\alpha_{3S}=0.60711$, $\alpha_5=6.17$, $\omega_3=-2$, $\omega_1=1$. The error of the approximation $E_F = 0.495375$.

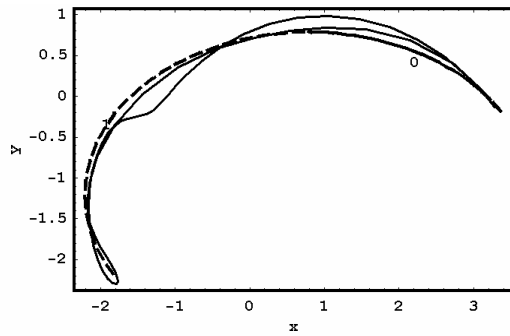


Figure 8. The arc of ellipse (dashed line - 0) and the curve generated by the mechanism (continuous line - 1).

The paper presents the first trial of the application of the F -function as a curve descriptor. The results obtained encourage further studies in this area.

7 Conclusions

The DCC method can be effectively applied in synthesis of complicated shapes, which is proved by the results of the synthesis of 2-DOF mechanism with nine optimized parameters. One can indicate some advantages over cumulative angle function and curvature, namely:

- no mathematical requirements but the continuity of the curve make the methods suitable for the description of non-smooth curves with straight segments and vertices,
- values of the DCC-function are limited, whereas in the case of curvature they may achieve high values,
- the simplicity of the mathematical definition,
- a small change in a shape results in a small change in the DCC function,
- the fast and simple normalization, the function itself is sensitive to the mirror reflection and starting point change only.

Moreover, the DCC function enables constructing the function invariant under affine transformations. The aim of the paper is to lay the foundations for further work. The problem can be extended by adding constraints on the admissible range of the transmission angle to minimize the forces transmitted by the links.

References

- Ullah, I., Kota, S. (1997). Optimal synthesis of mechanisms for path generation using Fourier descriptors and global search methods, *Journal of Mechanical Design* 119 504–510.
- Kunjur, A. and Krishnamuty, S. (1995). Genetic algorithm in mechanism synthesis, in: *ASME—Fourth Applied Mechanisms and Robotics Conference*, p. AMR 95-068-01-07.
- Cabrera, A.A., Simon, A. and Prado, M. (2002). Optimal synthesis of mechanisms with genetic algorithms, *Mechanism and Machine Theory* 37 1165–1177.
- Zahn, C.T. and Roskies, R.Z. (1972). Fourier descriptors for plane closed curves, *IEEE Transactions on Computers*, 21, 269-281.
- Ouyang, P. (2002). Force balancing design and trajectory tracking control of real-time controllable mechanisms, *M.Sc. thesis*, University of Saskatchewan.
- Rose, S. E. (1961). Five-bar loop synthesis, *Machine Design*, vol 33, pp. 189 - 195.
- Pollitt, E. P. (1962). Five-bar linkages with two drive cranks, *Machine Design*, vol 34, pp. 168 – 179.
- Laribi, M.A., Mlika, A., Romdhane, L. and Zeghloul, S. (2004). A combined genetic algorithm–fuzzy logic method (GA–FL) in mechanisms synthesis, *Mechanism and Machine Theory* 39, 717–735
- Vasiliu, A. and Yannou, B. (2001). Dimensional synthesis of planar mechanisms using neural networks: application to path generator linkages *Mechanism and Machine Theory* 36, 299-310
- Artobolovski, I. (1977) Theorie des mecanismes et des machines, *Edition MIR*, Moscou.
- Mayourian, M. and Freudenstein, F. (1984). The development of an atlas of the kinematic structures of mechanisms, *J. Mech. Trans. Automation Design* 106 (12), 458-461.
- Sandor, G.N. and Erdman, A.G. (1984). Advanced mechanism design analysis and synthesis, *Prentice-Hall, Englewood Cliffs, NJ*.
- McGarva, J. and Mullineux, G. (1993). Harmonic representation of closed curves, *Applied Mathematical Modelling* 17 213-218.
- McGarva, J. R. (1994). Rapid search and selection of path generating mechanisms from a library, *Mechanism and Machine Theory*, 29 (2), 223-235.
- Lu, K.J. and Kota, S. (2002). Compliant Mechanism Synthesis for Shape-Change Applications: Preliminary Results Smart Structures and Materials 2002: *Modeling, Signal Processing, and Control*, Vittal S. Rao, Editor, *Proceedings of SPIE*, vol. 4693.
- Mundo, D., Gatti, G. and Dooner, D.B. (2007). Combined synthesis of five-bar linkages and non-circular gears for precise path generation, *12th IFToMM World Congress*, Besançon (France), June 18-21.
- Kindratenko, V.V. (2003) On using functions to describe the shape, *Journal of Mathematical Imaging and Vision* 18: 225–245.
- Chanussot, J., Nystro, I. and Sladoje .N. (2005). Shape signatures of fuzzy star-shaped sets based on distance from the centroid, *Pattern Recognition Letters* 26 735–746.
- Feng, G., Xiao-Qiu, Z., Yong-Sheng, Z., Hong-Rui, W. (1996). A physical model of the solution space and the atlas of the reachable workspace for 2-dof parallel planar manipulators, *Mechanism and Machine Theory* 31 2, 173-184.
- Dibakar, S. and Mruthyunjaya, T.S. (1999). Synthesis of workspaces of planar manipulators with arbitrary topology using shape representation and simulated annealing, *Mechanism and Machine Theory* 34, 391–420.